Algerian Journal of Environmental Science and Technology
December edition. Vol.7. Nº4. (2021)
ISSN : 2437-1114
www.aljest.org

Estimation of global solar radiation using adaptive neuro-fuzzy inference system

D. Benatiallah [1]*, K. Bouchouicha [2] , A. Benatiallah [1], A.Harouz[1], B. Nasri[1]

[1]Laboratory of Sustainable Development and Computer Science (LSDCS), Faculty of Sciences and Technology University Ahmed Draia, Adrar, 01000, Algeria
[2]Unité de Recherche en Energies Renouvelables en Milieu Saharien (URER.MS)- Adrar-Algeria

*Corresponding author: djelloulunv@gmail.com ; Tel.: +213 662 11 79 03

ARTICLE INFO

Article History :

Received ***: 04/02/2020***
Accepted ***: 25/07/2020***

***Key Words*:**

ANFIS;
Solar radiation;
Intelligent system;
Solar energy;
sky-condition;
Neuro-fuzzy.

ABSTRACT

Abstract: *In this paper, a hybrid intelligent system technique, named adaptive neuro-fuzzy inference system (ANFIS) has been used to estimate global solar radiation models under all sky condition. fifteen ANFIS based models were developed based on astronomical and meteorological parameters, namely, average air temperature (T_{avg}), relative humidity (RH), declination (DE), hour angle (HA) and extraterrestrial solar irradiation (H_0), during one year at four meteorological stations across different climatic regions of Algeria were considered. Models efficiency were evaluated using statistical tests, including mean bias error (MBE), root mean squared error (RMSE), mean absolute percentage error (MAPE), and coefficient of determination (R^2). The results showed that, the model 2 in the first scenario with input temperature average, relative humidity, hour angle and using the function gbellmf MFs offered the best combination for predicting global solar radiation compared to other models in all stations. This model can be used for heating, cooling and designing solar energy systems in arid and semi-arid climatic region when data are available.*

I. Introduction

Due to population and economic growth, the global demand for energy is growing rapidly, particularly in emerging market economies [1]. Exploitation of large-scale fusil fuels has endangered the environment by creating a series of serious problems such as climate change and air pollution. Hence, the use of renewable and sustainable sources of energy such as solar energy as a clean and free source, environmentally preferable has been adapted as an efficient way of reducing the above-mentioned hazardous threats [2-4]. Recognition of solar radiation is a prerequisite for design and optimization of solar energy systems inside a building, such as the applications of solar energy, agricultural modeling and illumination system, but it is not possible in many locations around the world and is generally predicted by readily available climate variables [5-8]. The national energy executed a large investment of the Algeria country plan for the utilization of renewable energy, which is expected to ensure 40% of energy needs by 2030 [9,10]. Due to its considerable cost, maintenance and calibration requirements, the majority of current stations in Algeria are not installed with solar radiation measuring instruments [11,12]. Solar researchers developed several empirical models for estimating solar radiation using different meteorological, astronomical and mathematical parameters as inputs, maximum and minimum air temperature, sunshine duration and relative humidity [13-18]. Ashrae (1985), [18] proposed the early model for estimating global, direct and diffuse solar radiation using zenith angle. During the previous years, various artificial intelligence algorithms have been used in many renewable energy applications for predicting the solar radiation, such as fuzzy logic (FL), artificial neural

networks (ANN), genetic algorithm (GA), and adaptive neuro-fuzzy inference system (ANFIS). Artificial neural networks (ANN) have been used by many authors to predict global solar radiation from meteorological data [19-25]. Rehman and Mohandas (2008) constructed three models of artificial neural networks in Saudi Arabia using different type's inputs as relative humidity, air temperature, day of the year and time day of the year, Benatiallah et al. (2020), [21] developed nine ANN models to predict global hourly solar radiation in Adrar city (Algeria), using some parameters of geographical and meteorological data input. Kumar et al. (2015), [26] developed a number of ANNs models to forecast global solar radiation. In this study, the ANN models had better results than the others techniques. In Tamilnadu (India), Sumithira et al. (2012), [27] carried out a comparative analysis between ANFIS and other soft computing techniques model to estimate global solar radiation. They found that the ANFIS model performed better compared to other literature models. Olatomiwa et al. (2015), [28] evaluated the performances of deferent models including ANFIS models for estimation of global solar radiation in an area of Nigeria. In the paper of Kaushika et al. (2014), [19] used artificial intelligence models to forecast direct, diffuse and global solar radiations through clear sky conditions. Parameters such as mean hourly duration of sunshine, relative humidity and total rainfall data are used in Indian region. AI (Artificial intelligence) technique has been used by Yingni (2008), [29] to estimate solar radiation. Climate data used were collected from 9 china stations with different climatic conditions. Mohammadi et al. (2016), [25] applied the adaptive neuro-fuzzy inference system (ANFIS) to predict solar radiation in Kerman of Iran using different parameters of sunshine hour, extraterrestrial solar radiation and most influential parameters. In general the work focused on artificial intelligence for predicted solar radiation has shown higher performance than the empirical models.

In this paper, the artificial intelligence soft computing techniques named adaptive neuro-fuzzy inference system (ANFIS) is used to estimate global solar radiation. Depending on astronomical and meteorological, data set including extraterrestrial radiation, declination, hour angle, average air temperature and relative humidity have been used as input data to estimate solar radiation value using ANFIS method. To determine most suitable input values that contribute to the estimation, fifteen models that include combination of different inputs have been obtained for each method. The mentioned data were collected from four sites in Algeria with different climate conditions (Adrar, Khenchela, El-Bayadh and El-Goléa) in the period of one-year.

II. Materials and methods

II.1. Study areas and data collection

The data used in this study is actual solar irradiance and meteorological parameters recorded at four measurments stations in different climatic regions of Algeria. The studied region covered is from 27° to 35°N and from 0°W to 7°E. The insolation time over theses region of the national territory exceeds 2000 hours annually and may reach a maximum of 3900 hours in the southern region. The daily obtained solar energy on a horizontal surface is 5 kWh/m^2 over the major part of the national territory (Fig. 1) or about 1700 kWh/m^2/year for the North and 2263 kWh/m^2/year for the South of the country [30].

According to first station, the measurements of global radiation were carried out in the Research Unit in Renewable Energy in Saharan Medium situated in the state of Adrar which consisted of SOLYS 2 system Kipp & Zonen CMP21 Pyranometer. The stations of El- Goléa, Khenchela and El-Bayadh measurements were performed using Kipp & Zonen CMP 6 Pyranometer through the Shariket Kahraba wa Taket Moutadjadida (SKTM). The characteristics of equipment used are listed in Table 2. Whose measurement quality has been checked in the present study by simple quality control procedures in order to improve the obtained results either data initially lacking or removed via quality checks [31-33]. The physical limit of test processes were applied to the global solar irradiance (W/m^2) using the horizontal surface values of extraterrestrial irradiance. According to the outcomes of quality controls, the omission data represent no more than 1% at each station except for Adrar station the missing measurements represent around 3% of database.

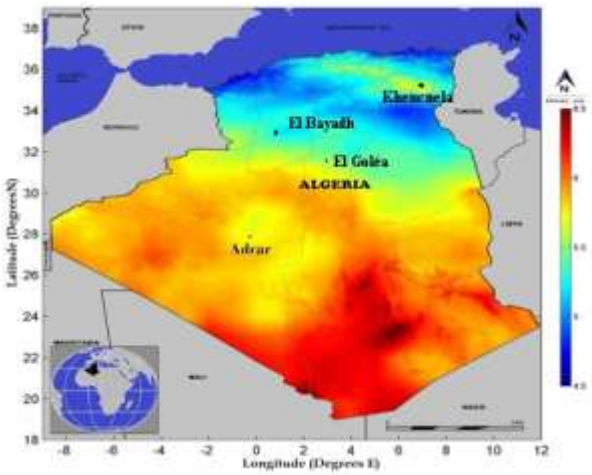

Figure1.*Annual map of global horizontal solar radia tion in Algeria*

The data solar irradiation measurements recorded from January to December 2016. The dataset consists of averaged 10 minutes interval value.

Algerian Journal of Environmental Science and Technology
December edition. Vol.7. Nº4. (2021)
ISSN : 2437-1114
www.aljest.org

Table1.*Geographical details of the measuring sites s elected*

Station	Site	Longitude	Latitude	Altitude (m)
Station 1	Adrar	0° 28' W	27° 88' N	269
Station 2	Khenchela	7° 08′ E	35° 25′ N	1121
Station 3	El-Bayadh	1° 01′ E	33° 41′ N	1304
Station 4	El-Goléa	2° 87' E	30° 58' N	380

Table 2. *Characteristics of solar instruments*

Sensor	*Kipp & Zonen CMP21*	*Kipp & Zonen CMP 6*
Maximum operational irradiance	4000 W/m^2	2000 W/m^2
Spectral range	270 to 3000 nm	285 to 2800 nm
Sensitivity	7 to 14 µV/W/m^2	5–20 µV/W/m^2
Directional response	<10 W/m^2	<20 Wm^{-2}
Non-stability	<0.5%	0.5%
Temperature	<1% (−20° to +50°)	4% (0° to +100°)
Response time	<5 s	18 s
Non-linearity	<0.2 %	0.5%
Operating and storage temperature	−40° to +80°	−40° to +80°

II.2.ANFIS based model to estimate global solar energy

The Adaptive neuro fuzzy inference system (ANFIS) is a hybrid artificial intelligence technique composed of artificial neural network and fuzzy logic. This technique is a flexible method that allows users to add prior knowledge into a neural network as a rule and has the ability to capture the non linear structure of a process and very fast convergence. This uses the least squares method combined with the gradient descent method to adjust the system parameters. This method is based on the use (Fig. 2) of multilayer networks [34].

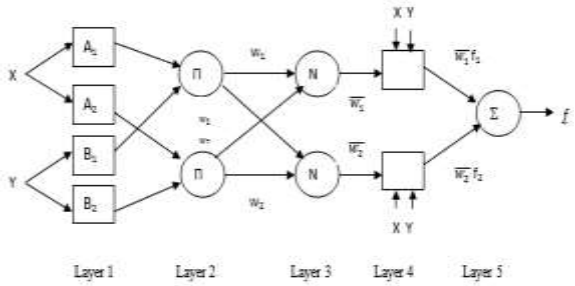

Figure 2. *Basic structure of ANFIS*

The fuzzy inference method has two x and y inputs, and one z output

The basic rule contains two fuzzy "if-then" rules of the Takagi Sugeno type:

• Rule 1. If x is A_1 and y is B_1, then $f_1 = p_1x + q_1y + r_1$ (1)

• Rule 2. If x is A_2 and y is B_2, then $f_2 = p_2x + q_2y + r_2$ (2)

where x and y are the crisp inputs to node i, A_i and B_i are the fuzzy sets in the antecedent, f_i is the output within the fuzzy region specified by the fuzzy rule; and p_i, q_i and r_i are the design parameters that are determined during the training process [20].

ANFIS has an architecture composed of five layers as shown in Fig. 2, and the following describes the structure [35]:

Layer 1. (Fuzzy layer):

• $O_{l,i}$ is the output of the *i*th node of the layer *l*.

• Every node *i* (indicated by a square) in this layer is an adaptive node with a node function

$O1,i = \mu_{Ai}(x)$ for $i = 1, 2$, or (3)

$O1,i = \mu_{Bi-2}(x)$ for $i = 3, 4$ (4)

• x (or y) is the input node *i* and A_i (or B_{i-2}) is a linguistic label associated with this node

• Therefore $O_{1,i}$ is the membership grade of a fuzzy set (A_1,A_2,B_1,B_2).

Typical membership function (MF's). The MF's can take any form of function (Gaussian, triangle, trapezoidal, etc); such that the generalized functions of these forms are indicate in Table 3.

Table 3. *Different basic MF's used in the study*

Membership functionf MFs	*Equation*	
Triangular MF	$\mu_{Ai}(x) = \max\left(\min\left(\frac{x-a}{b-a}, \frac{c-x}{c-b}\right), 0\right)$	(5)
Trapezoidal MF	$\mu_{Ai}(x) = \max\left(\min\left(\frac{x-a}{b-a}, 1, \frac{d-x}{d-c}\right), 0\right)$	(6)
Gaussian MF	$\mu_{Ai}(x) = \exp\left(-\frac{(x-c)^2}{2\sigma^2}\right)$	(7)
Bell-Shaped MF	$\mu_{Ai}(x) = \frac{1}{1+\left\|\frac{x-c}{a}\right\|^{2b}}$	(8)
Pi-shaped MF	$\mu_{Ai}(x;a,b,c,d) = \begin{cases} 0, & x \le a \\ 2\left(\frac{x-a}{b-a}\right)^2, & a \le x \le \frac{a+b}{2} \\ 1-2\left(\frac{x-a}{b-a}\right)^2, & \frac{a+b}{2} \le x \le b \\ 1, & b \le x \le c \\ 1-2\left(\frac{x-c}{d-c}\right)^2, & c \le x \le \frac{c+d}{2} \\ 2\left(\frac{x-d}{d-c}\right)^2, & \frac{c+d}{2} \le x \le d \\ 0, & x \ge d \end{cases}$	(9)

a, b, c, d is the parameter set, those parameters are referred to as premise parameters which changes the shapes of the MFs with maximum 1 and minimum 0.

Layer 2. (Product layer):
• Every node in this layer is a circle node labeled *Prod* denoted with Π
• The output is the product of all the incoming signals.
• $O_{2,i} = w_i = \mu_{Ai}(x) \,.\, \mu_{Bi}(y)$, for i = 1, 2 (10)
• Each node represents the fire strength of the rule
• Any other T-norm operator that perform the *AND* operator can be used.

Layer 3. (Normalized layer):
• Every node in this layer is a fixed node labeled *Norm* represented with N in Fig. 2.
• The *i*th node calculates the ratio of the *i*th rulet's firing strenght to the sum of all rulet's firing strengths.

• $O_{3,i} = \overline{w_i} = \frac{w_1}{w_1+w_2}$, i = 1, 2 (11)
• Outputs are called normalized firing strengths.

Layer 4. (De-fuzzy layer):
• Every node *i* in this layer is an adaptive node with a node function:

$O_{4,i} = \overline{w_i}\, f_i = \overline{w_i}\,(p_i x + q_i y + r_i)$, for i=1, 2. (12)

• $\overline{w_i}$ is the normalized firing strenght from layer 3, and $\{p_i, q_i, r_i\}$ is the parameter set of this node.
• These parameters are referred to as consequent parameters.

Layer 5. (Total output layer):
• The single node in this layer is a fixed node denoted with Σ, which computes the overall output as the summation of all incoming signals:

•*Estimated overall output* = $O_{5,1} = \sum_i \overline{w}_i . f_i = \frac{\sum_i w_i f_i}{\sum_i w_i}$ (13)

II.3. Hybrid Learning Algorithm

The ANFIS use a hybrid learning algorithm to calculate the premise and consequent parameters. The algorithm uses the least-square method in the forward pass to define the consequent parameters on layer 4. The errors are propagated backwards in the backward pass, and the premise parameters are modified by gradient descent (show Table 4). Usually, this error calculation is defined by the sum of the square difference between measured and estimated values and is minimized to a desired value.

Table 4. *The ANFIS hybrid learning algorithm contains two passes*

	Forward Pass	***Backward Pass***
Premise Parameters	Fixed	Gradient Descent
Consequent Parameters	Least-squares estimator	Fixed
Signals	Node outputs	Error signals

The final global output *f* in Fig. 2 can be represented as linear combinations of the corresponding parameters and rewritten as follows:

$f = (\overline{w_1}.\, x)\, p_1 + (\overline{w_1}.\, y)\, q_1 y + (\overline{w_1})\, r_1 + (\overline{w_2}.\, x)\, p_2 + (\overline{w_2}.\, y)\, q_2 y + (\overline{w_2})\, r_2$ (14)

where x and y are the input parameters, w_1, w_2 are the normalized firing strengths and p_1, q_1, r_1, p_2, q_2, r_2 are the parameters set.
For this ANFIS technique we developed computer programs using a script file written in the MATLAB software® V. 2014b in the four locations; Adrar, Khenchela, El-Bayadh and El-Goléa.
We worked with the meteorological and astronomical parameters (see Table 5) to predicted the global solar radiation (H)) output and as input: average Temperature (T_{avg}), Relative Humidity (RH), and calculates the parameters: hourly declination (δ), Hour Angle (HA), extraterrestrial radiation (H_0) [36], according to the equations (15-17) respectively:

$\delta = 23.45 \sin\frac{360}{365}(j + 284)$ (15)

$H_0 = \frac{24}{\pi}\, g_0 \left(\cos(\theta)\cos(\delta)\sin(w) + \sin(\theta)\sin(\delta)\frac{\pi}{180} w\right)$ (16)

HA= 15.*(TSV-12) (17)

With j number days of the year (from 1 to 365), and TSV is True Solar Time.

Table 5. *The input parameters used in the calculation*

Parameters	*Abbreviation*	*Unit*	*Category*
Average Temperature	T_{avg}	°C	Meteorological
Relative Humidity	RH	%	
Declination	DE	Degree	Astronomical
Hour Angle	HA	Degree	
Extraterrestrial solar irradiation	H_0	Wh/m^2	

For this analysis three scenarios through 15 models were evaluated by taking into account the inputs T_{avg}, RH, HA, Declination and H_0 with five membership functions trapmf, gbellmf, pimf, trimf, gaussmf: (1) T_{avg}, RH and HA were used for model 1 to model 5; (2) T_{avg}, RH and Declination were used for model 6 to model 10; (3) T_{avg}, RH and H_0 were used for model 11 to model 15. To determine its influence on the models, the T_{avg}, RH measured parameters, and one of the five MFs were included for all models and scenarios. Table 6 describes the structured parameters for the training of the ANFIS models.
To avoid the risk of overfitting, all data in the experimental dataset were standardized to the range from zero to one. Furthermore, to ensure the representativeness of the dataset, the database was randomly divided into two subsets, using 80 percent

for training, and the remaining 20 percent for validating the model. The training data set is being used to train all models and the validation data set was used to test the perfor mance of the trained models.

Table 6. *Different models used for ANFIS training*

Models	*Input parameters*					*membership functions*				
	T_{avg}	RH	HA	DE	H_0	trapmf	gbellmf	pimf	trimf	gaussmf
Model 1	X	X	X			X				
Model 2	X	X	X				X			
Model 3	X	X	X					X		
Model 4	X	X	X						X	
Model 5	X	X	X							X
Model 6	X	X		X		X				
Model 7	X	X		X			X			
Model 8	X	X		X				X		
Model 9	X	X		X					X	
Model 10	X	X		X						X
Model 11	X	X			X	X				
Model 12	X	X			X		X			
Model 13	X	X			X			X		
Model 14	X	X			X				X	
Model 15	X	X			X					X

II.4 Model Statistical Evaluation

The performance of the considered ANFIS models was evaluated using tests commonly used in evaluation scores [37], such as Root Mean Square Error (RMSE), Mean Bias Error (MBE), Mean Absolute Percentage Error (MAPE), and coefficient of determination (R^2).
These statistical tests are specified by the following equations (18–21).

$$RMSE = \sqrt{\frac{1}{n}\sum\left(G_c^i - G_m^i\right)^2} \quad (18)$$

$$MBE = \frac{1}{n}\sum\left(G_c^i - G_m^i\right) \quad (19)$$

$$MAPE = \frac{100}{n}\sum\left|\frac{\left(G_c^i - G_m^i\right)}{G_m^i}\right| \quad (20)$$

$$R^2 = \frac{\sum\left(G_c^i - C_{c,avg}\right)\left(G_m^i - C_{m,avg}\right)^2}{\sum\left(G_c^i - C_{c,avg}\right)^2 \sum\left(G_m^i - C_{m,avg}\right)^2} \quad (21)$$

where G_c^i : is the i^{th} estimated value
G_m^i : is the i^{th} measured value
$C_{m,avg}$: is the average of the estimated values
$C_{m,avg}$: is the average of the measured values
n: is the total number of data points

MBE (W/m^2) offers long-term output information for the models. The RMSE (W/m^2) test gives details about model success in the short term. Smaller RMSE and MBE values mean a better approximation of the models to the calculated values, a zero value is ideal. The MAPE is an overall predictability measure and is calculated from the absolute differences between a series of estimated and measured data. R^2 Takes the values 0 to 1 and suggest a closer matching of the model results to patterns in the measured data. RMSE and MBE are commonly used basic metrics for the performance evaluation of estimation models [38].

III. Results and discussion

In this study, four meteorological stations located in Algeria used the ANFIS computing technique for prediction of global solar radiation. For both training and testing data sets the statistical output indicators for each model are listed in Table 7. This table illustrated the Mean Bias Error, Root Mean Square Error, and coefficient of determination. Interestingly, the best model to use for estimation gives the best approximation with the measured data. The results of overall average statistical of MAPE, MBE, rMBE, RMSE, rRMSE and R for all scenario and models are reported in Table 8 and Fig. 3. In general, all models used in this study performed well in estimating global solar radiation.
In the first scenario (Table 8 and Fig. 3), when T_{avg}, RH, HA, data are included and gbell membership function is used, the model 2 achieved the best performance for all models in the testing phase according to mean performance statistics (R^2=0.9965, RMSE=19.37 Wh/m^2/day and MBE=0.0001 Wh/m^2/day), followed by Model 5 (R^2=0.9951, RMSE=22.85 Wh/m^2/day and MBE=0.0003

Wh/m^2/day). In the second scenario, the model 7 with inputs of T_{avg}, RH, declination and by using membership function gbell performed the best for all models according to overall mean errors (R^2=0.9159, RMSE=90.70 Wh/m^2/day and MBE=0.0017 Wh/m^2/day), followed by model 10 (R^2=0.9091, RMSE=93.88 Wh/m^2/day and MBE= -0.0002 Wh/m^2/day).

Table 7. *Statistical scores of RMSE, MBE and R^2 for each model during training and testing phases on four locations*

Station/Model	Training data			Testing data		
	R^2	RMSE (Wh/m^2)	MBE (Wh/m^2)	R^2	RMSE (Wh/m^2)	MBE (Wh/m^2)
Adrar						
Model 1	0.9851	38.9842	0.0001	0.9892	33.0604	0.0004
Model 2	0.9950	22.5211	0.0002	0.9975	15.8690	-0.0003
Model 3	0.9876	35.5483	-0.0008	0.9894	32.8179	0.0001
Model 4	0.9878	35.3041	0.0001	0.9937	25.4115	-0.0001
Model 5	0.9933	26.1569	-0.0003	0.9951	22.4398	0.0007
Model 6	0.9453	73.8880	0.0007	0.9508	70.0449	0.0005
Model 7	0.9597	63.6466	0.0008	0.9603	63.0181	0.0001
Model 8	0.9452	73.9374	-0.0005	0.9494	70.9519	-0.0001
Model 9	0.9637	60.4633	0.0003	0.9664	58.0782	0.0002
Model 10	0.9568	65.8171	-0.0004	0.9593	63.8340	0.0002
Model 11	0.9805	44.3624	-0.0005	0.9838	40.5810	0.0003
Model 12	0.9903	31.3631	0.0029	0.9910	30.2311	0.0003
Model 13	0.9789	46.2062	-0.0004	0.9837	40.7018	0.0003
Model 14	0.9878	35.1415	-0.0001	0.9866	36.9925	0.0002
Model 15	0.9887	33.8348	-0.0026	0.9920	28.5124	-0.0006
Khenchela						
Model 1	0.9856	30.3884	0.0001	0.9871	28.8648	0.0001
Model 2	0.9984	10.3138	0.0001	0.9989	8.3051	0.0001
Model 3	0.9845	31.5963	-0.0002	0.9861	29.9283	0.0001
Model 4	0.9953	17.4179	0.0001	0.9956	16.8058	-0.0001
Model 5	0.9978	12.0518	0.0002	0.9989	8.5506	0.0001
Model 6	0.7992	108.2341	0.0001	0.8102	105.4488	0.0002
Model 7	0.8428	96.9284	0.0001	0.8857	83.5651	0.0005
Model 8	0.8091	105.8184	-0.0003	0.8170	103.7520	-0.0001
Model 9	0.8462	95.8799	-0.0002	0.8556	93.2113	0.0004
Model 10	0.8365	98.6874	0.0011	0.8754	87.0131	-0.0006
Model 11	0.9856	30.3787	0.0004	0.9847	31.3931	0.0013
Model 12	0.9934	20.6894	-0.0169	0.9937	20.0951	0.1447
Model 13	0.9834	32.6035	0.0026	0.9831	32.9711	0.0015
Model 14	0.9917	23.1060	-0.0411	0.9909	24.1873	-0.0131
Model 15	0.9942	19.3232	-0.0138	0.9948	18.2821	-0.0115
El-Bayadh						
Model 1	0.9657	88.1176	0.0002	0.9632	91.0124	-0.0001
Model 2	0.9855	57.7235	0.0008	0.9909	45.5983	0.0004
Model 3	0.9602	94.8031	0.0001	0.9608	93.9021	0.0001
Model 4	0.9730	78.3101	-0.0001	0.9769	72.3844	0.0001
Model 5	0.9807	66.4606	0.0005	0.9885	51.1420	0.0001
Model 6	0.8138	197.3054	0.0002	0.8063	200.3611	-0.0002
Model 7	0.8630	171.5867	0.0001	0.8590	173.4809	0.0068
Model 8	0.8154	196.5716	-0.0015	0.8039	201.4434	0.0017

Model 9	0.8026	202.5526	-0.0008	0.8164	195.5964	0.0001
Model 10	0.8646	170.6505	-0.0007	0.8473	179.9509	0.0005
Model 11	0.9586	96.6618	0.0007	0.9664	87.1040	0.0007
Model 12	0.9736	77.4663	0.0181	0.9735	77.5314	-0.0391
Model 13	0.9552	100.4935	-0.0009	0.9604	94.4143	-0.0015
Model 14	0.9652	88.8124	-0.0225	0.9685	84.3608	-0.0053
Model 15	0.9767	72.9590	-0.0627	0.9788	69.3668	0.1495
El-Goléa						
Model 1	0.9777	31.7336	0.0001	0.9809	29.1840	0.0001
Model 2	0.9977	10.3094	0.0001	0.9987	7.7254	0.0001
Model 3	0.9760	32.8710	0.0003	0.9776	31.5333	0.0001
Model 4	0.9940	16.5774	0.0001	0.9932	17.4896	0.0001
Model 5	0.9966	12.4347	0.0002	0.9981	9.2832	0.0003
Model 6	0.9450	49.3588	0.0004	0.9449	49.0868	-0.0004
Model 7	0.9691	37.2993	-0.0015	0.9586	42.7382	-0.0004
Model 8	0.9397	51.6153	-0.0001	0.9396	51.3447	-0.0002
Model 9	0.9548	44.8523	0.0001	0.9407	50.8674	0.0001
Model 10	0.9655	39.3229	0.0001	0.9545	44.7540	-0.0002
Model 11	0.9795	30.4079	0.0019	0.9814	28.7743	-0.0008
Model 12	0.9935	17.1654	-0.0006	0.9960	13.4572	-0.0016
Model 13	0.9806	29.5767	0.0046	0.9782	31.1240	0.0064
Model 14	0.9813	29.0933	0.0058	0.9847	26.1675	-0.0002
Model 15	0.9938	16.8493	-0.0042	0.9952	14.7192	-0.0016

In the third scenario, when T_{avg}, RH, H_0, data are included and gaussmf is used, the model 15 achieved the best performance for all models in the testing phase according to score performance statistics (R^2=0.9902, RMSE=32.72 Wh/m^2/day and MBE=0.0340 Wh/m^2/day). The model 12 had a similar performance to the model 15 (R^2=0.9886, RMSE=35.32 Wh/m^2/day and MBE=0.0261 Wh/m^2/day). From Figure 3, when simulated between the estimated and measured data; it is evident that for the scenario 1 and 3, the MAPE were less than 6 % and 7%, respectively, and for the scenario 2 the MAPE ranging from 14-18%. The lowest value of MAPE coefficients registered in all scenarios is related to the model 2 (MAPE < 3%). Therefore, rRMSE did not exceed the percentages of 12, 28 and 13%, for the scenarios 1, 2 and 3, respectively.

Table 8. *Overall average statistical scores of RMSE, MBE and R^2 for each model during testing phases*

Overall average	Model	MBE (Wh/m^2)	rMBE (%)	RMSE (Wh/m^2)	R^2
Scenarios 1	Model 1	0.0002	0.0002	45.5304	0.9801
	Model 2	**0.0001**	**0.0001**	**19.3745**	**0.9965**
	Model 3	0.0002	0.0002	47.0454	0.9785
	Model 4	0.0002	-0.0002	33.0228	0.9898
	Model 5	0.0003	0.0008	22.8539	0.9951
Scenarios 2	Model 6	0.0001	0.0001	106.2354	0.8780
	Model 7	**0.0017**	**0.0003**	**90.7006**	**0.9159**
	Model 8	0.0003	0.0004	106.8730	0.8775
	Model 9	0.0001	0.0004	99.4383	0.8948
	Model 10	-0.0002	-0.0005	93.8880	0.9091
Scenarios 3	Model 11	0.0004	0.0014	46.9631	0.9791

	Model 12	0.0261	0.0135	35.3287	0.9886
	Model 13	0.0016	0.0005	49.8028	0.9764
	Model 14	-0.0046	-0.0016	42.9270	0.9827
	Model 15	**0.0340**	**0.0049**	**32.7201**	**0.9902**

In all cases, the first scenario models with hour angle input have an excellent performance than the second and the third scenario models (Table 7, Table 8 and Fig. 3).Thus the model 2 in the first scenario, according to the statistical indicators, when T_{avg}, RH, and HA, data are included, provided the best accuracy than the models of second and third scenarios (MAPE =2.04, rRMSE=4.41, rMBE=0.0001 and R^2=0.9965). Additionally, the role of gbell MFs had a positive impact on model output when prediction of global solar irradiance of the four stations. In general, extraterrestrial solar based models (scenario 3) were less accurate compared to models that used hour angle (scenario 1). Whereas models of scenario 2 that use declination had the worst performance (Table 8 and Fig. 3).

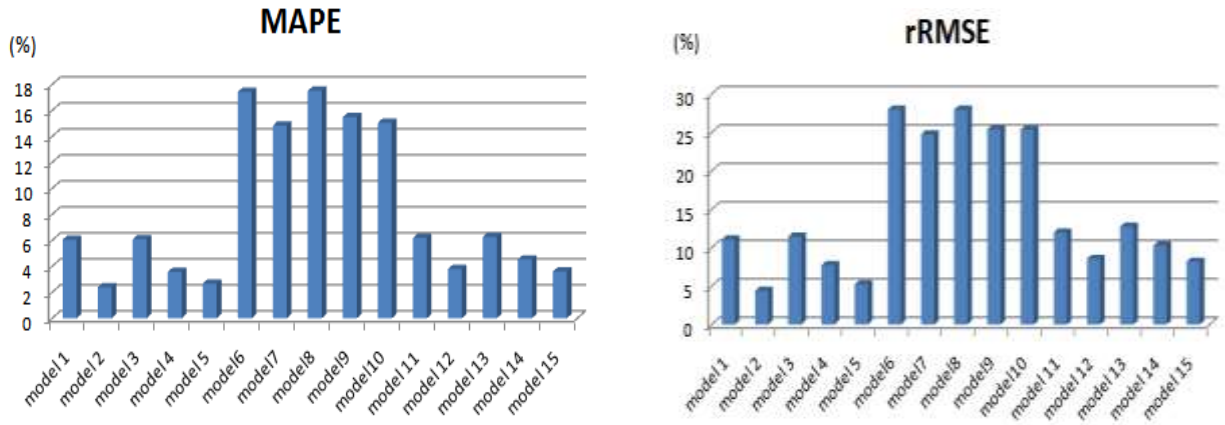

Figure 3. *MAPE and rRMSE model during testing phases*

During the training and testing process the statistical results for the data set are shown in Table 7. The output indicators demonstrate the dominance of model 2 in scenario 1 over scenario 2 and scenario 3. Fig. 4 also shows the scatter plots of estimated daily solar global radiation values by the model 2 (best model) for the testing phase in the four meteorological stations. It can be shown that the data are distributed as a series of points closer to the linear (red) perfect fit, indicating the relationship between measured and estimated values at each station over the study period. Furthermore, the results are generally consistent with the studies published recently. That mainly concluded that ANFIS technique offers a very reliable estimation of the solar radiation [39-41]. Also were compared to the proposed model with nominated models in literature which are relevant to the location of the study [42-44], the results obtained based on this model presented in current study in satisfactory agreement compared it with the existed models in the literature.

.

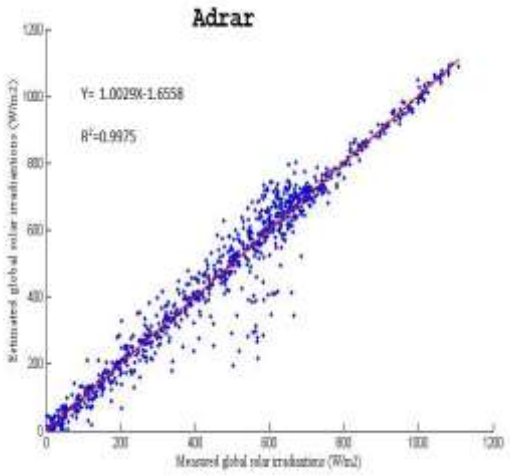

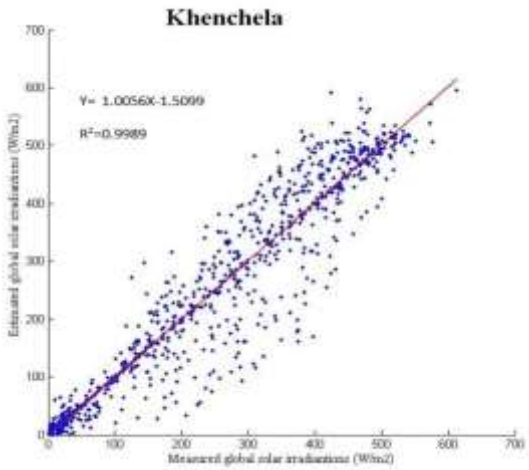

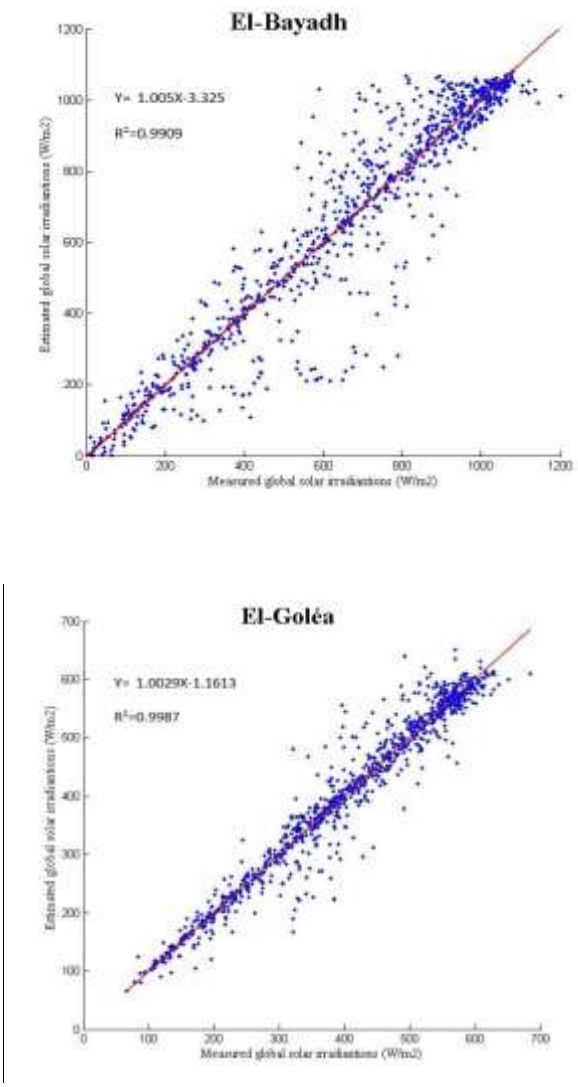

***Figure 4**. Scatter plot for the ANFIS model between measured and estimated values of daily global solar radiation during test phase*

IV. Conclusions

Estimation of solar radiation properly has a vital role in the renewable and sustainable energy sector for better decision making. In the present study, an adaptive neuro-fuzzy inference system (ANFIS) based model was applied for global solar radiation prediction at four locations in different regions of Algeria. Combination of T_{avg}, RH, DE, HA and H_0 was used in fifteen ANFIS structures to find the parameter that makes the best contribution to the prediction model. These structures include five membership functions associated with number of inputs. The solar irradiance prediction performance of ANFIS is investigated using different statistical indicators (R^2, RMSE, MBE and MAPE). The meteorological parameters as the air temperature, relative humidity and astronomical variables including hour angle, declination and extraterrestrial solar irradiation were used as the inputs of ANFIS models. The results indicated that the model 2 in the first scenario with input temperature average, relative humidity, hour angle and using the function gbell MFs has a slightly better performance than other mentioned models in total. Finally, these results show that the presented models are a useful alternative method for solar radiation prediction, which can play an important role in design and installation of solar PV and Thermal Systems, and in buildings designation performance and capacity of these systems.

V. References

1. Junliang, F.; Xiukang, W.; Fucang, Z.; Xin, M.; Lifeng, W. Predicting daily diffuse horizontal solar radiation in various climatic rons of China using support vector machine and tree-based soft computing models with local and extrinsic climatic data. *Journal of Cleaner Production* (2019).
2. Khorasaninejad, E.; Hajabdollahi, H. Thermo-economic and environmental optimization of solar assisted heat pump by using multi-objective particle swam algorithm. *Energy* 72 (2014) 680-90.
3. Rizwan, M.; Jamil, M.; Kirmani, S.; Kothari, D. Fuzzy logic based modeling and estimation of global solar energy using meteorological parameters. *Energy* 70 (2014) 685-91.
4. Casares, F.; Lopez-Luque, R.; Posadillo, R.; Varo-Martinez, M. Mathematical approach to the characterization of daily energy balance in autonomous photovoltaic solar systems. *Energy* 72 (2014) 393-404.
5. Piri, J.; Shamshirband, S.; Petkovic, D.; Tong, C.; Rehman, M. Prediction of the solar radiation on the Earth using support vector regression technique. *Infrared Physics & Technology* (2014).
6. Benatiallah, D.; Benatiallah, A.; Bouchouicha, K. and Nasri, B. Estimation of clear sky global solar radiation in Algeria. *AIMS Energy* 7 (2019) 710–727.
7. Bouchouicha, K.; Hassan, M.; Bailek, N.; Aoun, N. Estimating the global solar irradiation and optimizing the error estimates under Algerian desert climate. *Renew Energy* 139 (2019) 844–858.
8. Bouchouicha, K.; Bailek, N.; Mahmoud, M.; Alonso, J.; Slimani, A.; Djaafari, A. Estimation of monthly average daily global solar radiation using meteorological-based models in Adrar, Algeria. *Appl Sol Energy* 54 (2018) 448–455.
9. Stambouli, A.; Khiat, Z.; Flazi, S.; Kitamura, Y. A review on the renewable energy development in Algeria: current perspective, energy scenario and sustainability issues. *Renew Sustain Energy Rev*. 16 (2012) 4445–4460.
10. Bailek, N.; Bouchouicha, K.; Yasser, A.; El-Shimy, A.; Slimani, A.; Basharat, J. & Djaafari, A. Developing a new model for predicting global solar radiation on a horizontal surface located in Southwest Region of Algeria. *NRIAG Journal of Astronomy and Geophysics*. 9 (2020) 341-349.
11. Bouchouicha, K.; Razagui, A.; Bachari, N.; Aoun, N. Mapping and geospatial analysis of solar resource in Algeria. *Int J Energy Environ Econ*. 23 (2015) 735–751.

12. Benatiallah, D.; Benatiallah, A., Bouchouicha, K. Model for obtaining the daily direct and diffuse solar radiations. International Journal of Science and Applied Information Technology 7 (2017) 50-55.
13. Jamil, B.; Akhtar, N. Estimation of diffuse solar radiation in humid-subtropical climatic region of India: comparison of diffuse fraction and diffusion coefficientmodels. Energy 131 (2017) 149–164.
14. Bakirci, K. Correlations for estimation of daily global solar radiation with hours of bright sunshine in Turkey. *Energy* 34 (2009) 485–501.
15. Benatiallah, D.; Benatiallah, A.; Hamouda, M.; Bouchouicha, K.; Harouz, A. Model R.Sun for obtaining the daily global solar. *International Journal of Science and Applied Information Technology* 7 (2017) 83-88.
16. Jamil, B.; Siddiqui, A. Generalized models for estimation of diffuse solar radiation based on clearness index and sunshine duration in India: applicability under different climatic zones. *J Atmos Solar-Terrestrial Phys*. (2017) 157–158.
17. Benatiallah, D.; Benatiallah, A.; Bouchouicha, K.; Hamouda, M. and Nasri, B. An empirical model for estimating solar radiation in the Algerian Sahara. American Institute of Physics. 7 (2018) 710–727.
18. Ashrae. Handbook of fundamentals. Atlanta, Georgia: American Society of Heating, *Refrigeration, and Air-Conditioning Engineers* (1985).
19. Kaushika, N.; Tomar, R.; Kaushik, S. Artificial neural network model based on interrelationship of direct, diffuse and global solar radiations. *Solar Energy* 103 (2014) 327-342.
20. Victor, H.; Javier, A.; Javier, A. and Laurel, S. ANFIS, SVM and ANN soft-computing techniques to estimate daily global solar radiation in a warm sub-humid environment. *Journal of Atmospheric and Solar–Terrestrial Physics* 155 (2017) 62–70.
21. Benatiallah, D.; Benatiallah, A.; Bouchouicha, K.; Nasri, B. Prediction du rayonnement solaire horaire en utilisant les reseaux de neurone artificiel. *Algerian J. Env. Sc. Technology*. 6 (2020) 1236-1245.
22. Kisi, O. Modeling solar radiation of Mediterranean region in Turkey by using fuzzy genetic approach. *Energy* 64 (2014) 429-36.
23. Dahmani, K.; Dizene, R.; Notton, G.; Paoli, C.; Voyant, C.; Nivet, M. Estimation of 5-min time-step data of tilted solar global irradiation using ANN (Artificial Neural Network) model. *Energy* 70 (2014) 374-81.
24. Rehman, S. and Mohandes, M. Artificial neural network estimation of global solar radiation using air temperature and relative humidity. *Energy Policy* 36 (2008) 571- 576.
25. Mohammadi, K.; Shamshirband, S.; Petković, D.; Khorasanizadeh, H. Determining the most important variables for diffuse solar radiation prediction using adaptive neuro-fuzzy methodology; case study: City of Kerman, Iran. *Renew. Sustain. Energy Rev*. 53 (2016) 1570–1579.
26. Kumar, R.; Aggarwal, R.; Sharma, J. Comparison of regression and artificial neural network models for estimation of global solar radiations. *Renew. Sustain. Energy Rev*. 52 (2015) 1294–1299.
27. Sumithira, T.; Kumar, A.; Rameshkumar, R. An adaptive neuro-fuzzy inference system (ANFIS) based prediction of solar radiation. *J. Appl. Sci. Res* 8 (2012) 346–351.
28. Olatomiwa, L.; Mekhilef, S.; Shamshirband, S.; Mohammadi, K.; Petković, D.; Sudheer, C. A support vector machine–firefly algorithm-based model for global solar radiation prediction. *Sol. Energy* 115 (2015) 632–644.
29. Yingni, J. Prediction of monthly mean daily diffuse solar radiation using artificial neural networks and comparison with other empirical models, *Energy Policy* 36 (2008) 3833–3837.
30. Benatiallah, D.; Benatiallah, A.; Harouz, A.; Bouchouicha, K. Development and Modeling of a Geographic Information System solar flux in Adrar, Algeria. *International Journal of System Modeling and Simulation*. 1 (2016) 15-19.
31. Journée, M.; Bertrand C. Quality control of solar radiation data within the RMIB solar measurements network. *Sol Energy* 85 (2011) 72–86.
32. Jiang, Y. Estimation of monthly mean daily diffuse radiation in China. *Appl. Energy* 86 (2009) 1458–1464.
33. Khorasanizadeh, H.; Mohammadi, K. Prediction of daily global solar radiation by day of the year in four cities located in the sunny regions of Iran. *Energy Convers. Manag*. 76 (2013) 385–392.
34. Jang, J. ANFIS: adaptive-network-based fuzzy inference system. *Syst. Man Cybern. IEEE Trans*. 23 (1993) 665–685.
35. Abdulshahed, A.; Longstaff, A.; Fletcher, S. The application of ANFIS prediction models for thermal error compensation on CNC machine tools. *Appl. Soft Comput*. 27 (2015) 158–168.
36. Allen, R.; Pereira, L.; Raes, D.; Smith, M. Crop Evapotranspiration-guidelines for Computing Crop Water Requirements-FAO Irrigation and Drainage Paper 56.FAO, Rome 300, 6541. (1998).
37. Stone, RJ. Improved statistical procedure for the evaluation of solar radiation estimation models, *Solar Energy* 51 (1993) 289–91.
38. Teke, A.; Yıldırım, H.; Çelik, Ö. Evaluation and performance comparison of different models for the estimation of solar radiation. *Renew. Sustain. Energy Rev*. 50 (2015) 1097–1107.
39. Perveen, G.; Rizwan, M.; Goel, N. An ANFIS-based model for solar energy forecasting and its smart grid application. Engineering Reports. (2019).
40. Muhammad, A.; Gaya, MS.; Aliyu, R. et al. Forecasting of global solar radiation using ANFIS and ARMAX techniques. *IOP Conf Ser Mater Sci Eng*. 303 (2018) 1-6.
41. Alparslan, N.; kayabaşi, A. and ruşen S. Estimation of Global Solar Radiation by Using ANN and ANFIS, Innovations in Intelligent Systems and Applications Conference (ASYU), Izmir, Turkey, (2019) 1-6.
42. Bouchouicha, K.; Bailek, N.; Bellaoui, M.; Oulimar, B. Estimation of Solar Power Output Using ANN Model: A Case Study of a 20-MW Solar PV Plan at Adrar, Algeria. *Lecture Notes in Networks and Systems*. (2020).
43. Oulimar, I.; Benatiallah, A.; Bouchouicha, K. Validation Modeles and Simulation of Global Horizontal Solar Flux as a Function of Sunshine Duality in Southern Algeria (Adrar). *Lecture Notes in Networks and Systems*. (2020).
44. Benatiallah, A.; Benatiallah, D.; Ghaitaoui, T.; Harrouz, A.; Mansouri, S. Modelling and Simulation of Renewable Energy Systems in Algeria, *International Journal of Science and Applied Information Technology* 7 (2017) 17-22.

Nomenclature

δ Déclinaison of the sun (°)
θ Latitude of station (°)
w Angle of solar height (°)
H_0 Extraterrestrial solar irradiation (W/m^2)
g_0 Coefficient of extraterrestrial solar radiation

Please cite this Article as:
Benatiallah D., Bouchouicha K., Benatiallah A., Harouz A., Nasri B., Estimation of global solar radiation using adaptive neuro-fuzzy inference system, ***Algerian J. Env. Sc. Technology***, ***7*:4 (2021) 2097-2106**